Chemical Engineering Journal 148 (2009) 394–404

Contents lists available at ScienceDirect

Chemical Engineering Journal

journal homepage: www.elsevier.com/locate/cej

Modelling of the synthetic dye Orange II degradation using Fenton's reagent: From batch to continuous reactor operation

J. Herney Ramirez, Filipa M. Duarte, F.G. Martins, Carlos A. Costa, Luis M. Madeira*

LEPAE – Departamento de Engenharia Química, Faculdade de Engenharia da Universidade do Porto, Rua Dr. Roberto Frias, 4200-465 Porto, Portugal

ARTICLE INFO

Article history:
Received 18 June 2008
Received in revised form 28 August 2008
Accepted 11 September 2008

Keywords:
Orange II
Kinetics
Fenton's reagent
Hydrogen peroxide
Oxidation

ABSTRACT

In this work, a simple kinetic model was used to study the azo dye Orange II (O-II) degradation using Fenton's reagent, in the Fenton-like stage. The effects of pH, temperature, Cl^- concentration and initial concentrations of O-II, hydrogen peroxide (H_2O_2) and ferrous ion catalyst (Fe^{2+}) on the degradation rate have been investigated in a batch reactor. The apparent kinetic constants, k_{ap}, for O-II degradation were determined in the following ranges of experimental conditions: $2.0 \leq pH \leq 4.0$, $283\,K \leq T \leq 323\,K$, $0\,M \leq C_{Cl^-} \leq 1 \times 10^{-2}\,M$, $3 \times 10^{-5}\,M \leq C_{OII_o} \leq 1 \times 10^{-4}\,M$, $1 \times 10^{-4}\,M \leq C_{H_2O_{2o}} \leq 1 \times 10^{-3}\,M$ and $2.5 \times 10^{-6}\,M \leq C_{Fe_o^{2+}} \leq 2 \times 10^{-5}\,M$. A pseudo first-order reaction rate with respect to O-II concentration was found to be adequate to fit the data in these experiments, in which k_{ap} depends on the initial conditions following a power-law dependency (at optimum pH of 3 and absence of chloride ions). This equation, without further fitting parameters, was successfully used to validate experiments performed in a continuous stirred tank reactor (CSTR). The ability of the model predictions was also checked by performing experiments in the CSTR out of the above-mentioned ranges (used for the kinetic study).

1. Introduction

Azo dyes are a class of synthetic dyes which make up 60–70% of all textile dyestuffs. These dyes are soluble in solution and are not removed via conventional biological treatments [1,2]. They can be divided into monoazo, diazo and triazo classes, according to the presence of one or more azo bonds (–N=N–) [3,4]. Some azo dyes and their precursors have been shown to be, or are suspected to be, human carcinogens as they form toxic aromatic amines [5–7]. In particular, Orange II (O-II), also called acid Orange 7, is a molecule with N=N bonds that is widely used in the dyeing of textiles and cosmetics, and thus found in the wastewaters of the related industries [8].

The processes used to decontaminate wastewater are physical, biological or chemical. The first do not lead to organics degradation but rather to their transfer from one phase to another. On the other hand, biological processes usually proceed at low rates and are very often inhibited by several substances, particularly those that inhibit or are toxic to the microorganisms, as is the case of many dyes. For these reasons, research efforts have been focused in developing attractive oxidation processes that might be employed as a pre-treatment stage (to increase organics biodegradability by partial oxidation) or as final treatment, in some cases for simple colour/dye removal. Recent progress in this field has led to the development of advanced oxidation processes (AOPs). Among them, oxidation using Fenton's reagent has proved to be a promising and attractive treatment method for the effective decolourization and degradation of dyes, as well as for the destruction of a large number of hazardous and organic pollutants [9–12]. Moreover, the process is simple, taking place at low temperatures and atmospheric pressure [13].

Oxidation with Fenton's reagent is based on ferrous ion and hydrogen peroxide and exploits the very high reactivity of the hydroxyl radical produced in acidic solution by catalytic decomposition of H_2O_2 – Eq. (1) [14]. The mechanism of Fenton's oxidation involves basically the following steps (Eqs. (1)–(6)), wherein kinetic constants reported are given in $M^{-1}\,s^{-1}$ (with the exception of k_5) and were taken from the literature [14–20]:

$$Fe^{2+} + H_2O_2 \rightarrow Fe^{3+} + HO^- + HO^\bullet, \quad k_1 = 51\text{–}100 \tag{1}$$

$$Fe^{2+} + HO^\bullet \rightarrow Fe^{3+} + HO^-, \quad k_2 = 3\text{–}4.3 \times 10^8 \tag{2}$$

$$Fe^{3+} + H_2O_2 \rightarrow Fe^{2+} + H^+ + HO_2^\bullet, \quad k_3 = 0.05\text{–}0.27 \tag{3}$$

$$H_2O_2 + HO^\bullet \rightarrow HO_2^\bullet + H_2O, \quad k_4 = 1.2\text{–}4.5 \times 10^7 \tag{4}$$

$$H_2O_2 \rightarrow 1/2O_2 + H_2O, \quad k_5 = 0.001\,s^{-1} \tag{5}$$

$$2HO^\bullet \rightarrow H_2O_2, \quad k_6 = 5.3 \times 10^9 \tag{6}$$

* Corresponding author. Tel.: +351 22 5081519; fax: +351 22 5081449.
E-mail address: mmadeira@fe.up.pt (L.M. Madeira).

1385-8947/$ – see front matter © 2008 Elsevier B.V. All rights reserved.
doi:10.1016/j.cej.2008.09.012

Nomenclature

A	pre-exponential coefficient of the kinetic law (s^{-1})
C_i	concentration of species i (M)
$C(t)$	Danckwerts' C curve (dimensionless)
$E(t)$	residence time distribution function (s^{-1})
E_a	apparent activation energy (kJ mol^{-1})
F_i	molar flow rate of species i (mol s^{-1})
k_{ap}	apparent kinetic rate constant (s^{-1})
k_i	rate constant for elementary Fenton reaction step i (M^{-1} s^{-1} or s^{-1})
Q	volumetric flow rate (L s^{-1})
$(-r_{OII})$	reaction rate for Orange II consumption (mol L^{-1} s^{-1})
R	ideal gas constant (J mol^{-1} K^{-1})
t	time (s)
T	temperature (K)
V	volume of reactor (L)
X	Orange II conversion (%)

Greek symbol

τ	space-time (s)

Subscripts

batch	batch reactor
Cl^-	chloride ion
exp	experimental conditions
Fe^{2+}	ferrous ion
H_2O_2	hydrogen peroxide
in	inlet conditions (continuous reactor)
mod	model prediction
o	initial conditions (batch reactor)
OII	Orange II
out	outlet conditions (continuous reactor)

Superscripts

a	reaction order with respect to Orange II concentration
b	reaction order with respect to H_2O_2 concentration
c	reaction order with respect to Fe^{2+} concentration
o	refers to initial conditions (continuous reactor – tracer experiments)

The $HO^\bullet$ species produced through reaction given by Eq. (1) will then attack organic matter present in the reaction medium, because such radical is a powerful inorganic oxidant that reacts non-selectively with numerous compounds (rate constants in the range 10^7–10^{10} M^{-1} s^{-1}) [14,21]:

$$OII + HO^\bullet \rightarrow \text{products} + H_2O \quad (7)$$

Several studies can be found in the literature dealing with the Fenton's process kinetics. However, due to the associated complexity (besides the above-mentioned many other reaction steps have to be taken into account), a phenomenological study requires a set of at least 20–30 differential equations. Even so, rate constants vary from work to work, and for several of them activation energies are not documented. Therefore, it is a main goal of the present work to find a simple semi-empirical equation that describes the kinetics of O-II degradation in a batch reactor by the Fenton's reagent, information that is required for modelling, design and optimization of chemical reactors used for the degradation of pollutants. The non-biodegradable azo dye Orange II was selected as model compound due to its wide application in several industries. Many operational parameters, such as pH, O-II concentration, H_2O_2 dosage, Fe^{2+} concentration and temperature, that affect the degradation efficiency, were investigated. The effect of Cl^- concentration on the oxidation efficiency was also studied because this species is usually present in textile effluents and is inhibitory for the Fenton's process. Finally, the kinetic law obtained was used to validate experiments carried out in a continuous reactor. To the best of the author's knowledge, there are available only a few studies about Fenton's reagent application in continuous reactors [e.g., 15,22,23], and none were found for the O-II dye. Studies dealing with the modelling of such continuous process are also scarce.

2. Materials and methods

Chemical oxidation of Orange II aqueous solutions was conducted in two stirred jacketed glass reactors; the first one was a batch while the second was a continuous stirred tank reactor (CSTR), with 0.30 L and 0.92 L capacity, respectively. In both cases temperature was controlled through a Huber thermostatic bath (Polystat CC1 unit). The reactors were equipped with a Falc F30ST magnetic stirrer for continuous stirring of the reaction mixture and a thermocouple was used to assess the temperature in the liquid phase. The absorbance and the pH were continuously monitored using a Philips PU8625 UV/VIS spectrophotometer and a pH-meter from EDT instruments (RE 357 TX), respectively. Data acquisition (at a frequency of 0.2 s^{-1}), with displaying and saving capabilities in a PC, was performed using a home-designed interface with software Labview 5.0, from National Instruments.

The dye, Orange II ($C_{16}H_{11}N_2NaO_4S$) from Fluka p.a., was used as received. In the batch runs, the initial pH was adjusted through addition of 1 M NaOH or 0.1 M H_2SO_4 to the dye solution. Then, solid iron sulphate ($FeSO_4{\cdot}7H_2O$, from Panreac) was added, followed by the hydrogen peroxide solution (30%, w/w, from Merck), with intermediate pH adjustment if necessary. Addition of H_2O_2 corresponds to the initial instant of the runs. For on-line absorbance measurements a flow-through cell was used, being the recirculation of the solution made with the help of a Watson-Marlow 5055 peristaltic pump at very high flow rate. This assembly allows an almost in-situ monitoring of the dye concentration in the reaction mixture, which, coupled with high data frequency acquisition, provided a good perspective of the concentration history. As discussed below, this allowed a better visualization of the change in the kinetics along the Fenton's process. Even so, not all the data are included in the figures, for a better visualization.

Orange II concentration was obtained from a calibration curve at the characteristic dye wavelength (486 nm), because this corresponds to the maximum of absorption and in this range interference by oxidation products does not occur [24].

For operation of the CSTR, the same peristaltic pump was used to feed two streams: one acidic containing the dye solution with the dissolved iron catalyst and another with the H_2O_2 solution. Both flow rates were carefully measured so that the concentration of each species, at the reactor inlet, was known. The exit stream was flowed through the spectrophotometer cell until a steady dye concentration was measured. All experiments were carried out at pH ~3.0. In experiments carried out in duplicate, conversion varied by less than 10% (relative error).

To obtain the residence time distribution in the continuous reactor, i.e., for studying the mixing characteristics in such a reactor, a tracer stimulus-response technique was used. The reactor was fed with distilled water and after being filled the tracer (O-II in this work) was suddenly added (pulse input with a syringe). Then, its concentration was measured along time in the outlet stream.

3. Results and discussion

3.1. Batch reactor – kinetic study

In the Fenton's process, it is generally considered that the reactions between hydrogen peroxide and ferrous iron in acidic medium involve the steps presented above (Eqs. (1)–(6)), although some authors propose a much more complex mechanism, with several other reactions and involving many radicals [e.g., 25]. In this process, formation of hydroxyl radicals was demonstrated by several researchers [26] and they have been suggested to be the main oxidant species. In spite of the oxidation kinetics complexity, it is often assumed that, under certain conditions, the process mechanism can be significantly simplified, being of particular relevance reaction (7) [26]. The corresponding kinetic equation (i.e., for reaction between O-II and HO•), assumed to be elementary, can thus be expressed as follows:

$$(-r_{OII}) = k_7 C_{HO\bullet} C_{OII} = k_{ap} C_{OII} \quad (8)$$

where k_{ap} is an apparent pseudo first-order kinetic constant that involves the radical HO concentration, assumed to remain constant along one experiment due to the hypothesis of a pseudo steady-state concentration of hydroxyl radicals. Such hypothesis was confirmed by solving the set of differential equations based on the above-mentioned reaction scheme, using the rate constants ranges reported in the literature. Besides, this approach is widely adopted in Fenton's oxidation studies [e.g., 25, 27–29]. The value of k_{ap} depends therefore on the initial reactants concentrations (H_2O_2 and Fe^{2+}), temperature, and also on the concentration of scavenger species present in the reaction mixture (such as intermediates, HOO•, etc.) [26]. On the other hand, these scavenger species concentrations depend on the initial O-II concentration, and for this reason k_{ap} is a function of all these variables [26]:

$$k_{ap} = f(C_{OII_o}, C_{H_2O_{2o}}, C_{Fe_o^{2+}}, T).$$

The dependence of k_{ap} from the operating conditions can be found by performing independent experiments, changing each factor at a time, after appropriate linearization of the data. This can be achieved starting from the corresponding mass balance in the batch reactor ($dC_{OII}/dt = -k_{ap}C_{OII}$, wherein the hypothesis of ideal mixing conditions has been verified by simple tracer experiments), thus yielding:

$$\ln \frac{C_{OII}}{C_{OII_o}} = -k_{ap} t \quad (9)$$

If the relationship between $\ln(C_{OII}/C_{OII_o})$ vs. time (t) is linear, then the degradation of O-II will follow a pseudo first-order reaction and the values of k_{ap}, at given experimental conditions, can be obtained from the slopes of these plots. However, the reaction exhibits a change on its kinetics, which is a consequence of the mechanism complexity. This has been widely reported in the literature associated with the Fenton's process, and for that reason k_{ap} values were calculated from experimental data covering only the Fenton-like phase of the process, this means where most of Fe^{2+} has been converted into Fe^{3+} (also called as stage II). Actually, it is known that the Fenton's process is divided in two-stage reactions. In the first organic compounds are decomposed rapidly and somewhat less rapidly in the second one. The main reason for this well-known behaviour is that ferrous ions react very quickly with hydrogen peroxide to produce large amounts of hydroxyl radicals (cf. Eq. (1) and corresponding rate constant), which can then react rapidly with the dye (so-called Fe^{2+}/H_2O_2 stage) [11]. Ferric ions produced can then react with H_2O_2 to produce hydroperoxyl radicals and restore ferrous ions (Eq. (3)). However, the rate of oxidation in the second stage (Fe^{3+}/H_2O_2 stage) is slower than in the first one due to the slow production of Fe^{2+} from Fe^{3+} [30]. Because the reaction in which Fe^{2+} is converted into Fe^{3+} is very fast, the first stage is short (or very short) and afterwards the process enters into a so-called pseudo steady-state, wherein Fe is mainly in the 3+ oxidation state.

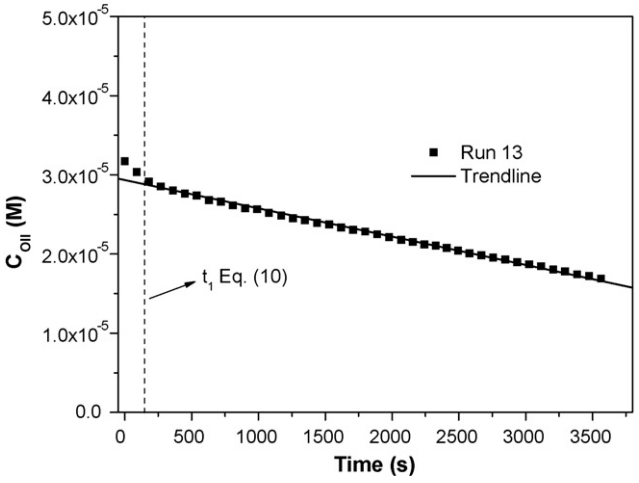

Fig. 1. Typical plot of the O-II concentration history. Experimental conditions: $C_{OII_o} = 1.1 \times 10^{-4}$M, $C_{H_2O_{2\,o}} = 2 \times 10^{-4}$M, $C_{Fe^{2+}} = 5 \times 10^{-6}$M, T = 303 K and pH 3.

Fig. 1 shows the transient O-II concentration curve in a typical experiment, evidencing clearly the existence of this two-stage process. For that reason the fitting of a single kinetic equation along all the process is not straightforward and so we used data only in the second stage of the process (pseudo steady-state, $t > t_1$). This means that, in general, about 90% of the experimental data in each run are used in the regression, and in all cases it is warranted that the conversion of Fe^{2+} into Fe^{3+} is higher than 95% (cf. Eq. (10), derived from Eq. (1), taking into account that H_2O_2 is present in large excess with respect to Fe^{2+}). In all experiments fitting of Eq. (9) to experimental data provided average relative errors below 6.5%, as described in the following section.

$$t_1 > -\frac{\ln\ 0.05}{k_1 C_{H_2O_2}} \quad (10)$$

3.2. Batch reactor – effect of the main operating conditions

In the closed reactor, several experiments on the dye degradation by Fenton's reagent were conducted by varying the temperature (283–323 K) and the initial concentrations of O-II (3×10^{-5} to 1×10^{-4} M), H_2O_2 (1×10^{-4} to 1×10^{-3} M) and Fe^{2+} (2.5×10^{-6} to 2×10^{-5} M). The effect of pH and of a scavenger usually present in textile effluents (chloride ion) was also analyzed.

3.2.1. Effect of the pH

The influence of initial pH in the degradation of O-II was first studied. Fig. 2 shows the fittings of Eq. (9) to the dye concentration data over time, showing clearly that O-II degradation in the Fenton-like stage (data in the first stage were omitted) fits well the pseudo first-order kinetic model (average relative error <1.0%), whatever is the reaction pH (in the range 2–4).

Table 1 shows the pH effect on the apparent kinetic constant (runs 1–4). It is evident that when the initial pH increases from 2 to 3 the value of k_{ap} quickly increases, decreasing drastically when the pH is raised from 3 to 4. This behaviour was observed by the authors previously [30] and agrees with literature findings, as it is usually accepted that acidic pH levels near 3 are usually optimum for Fenton oxidation [14,15,31]. At pH <3 the process becomes less effective. Indeed, in such conditions the regeneration of Fe^{2+}

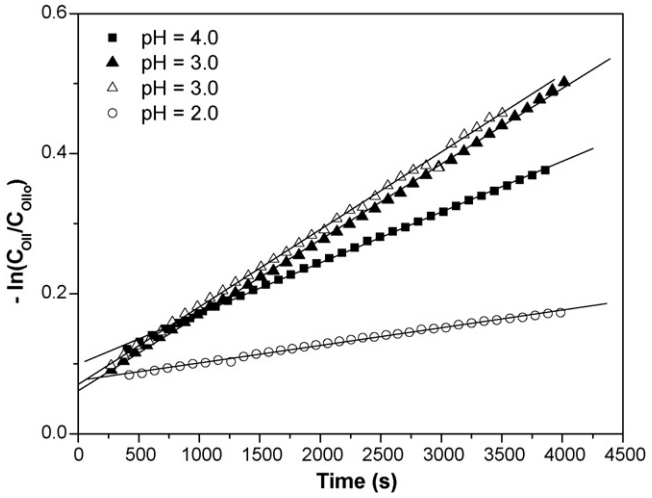

Fig. 2. Linearized dye concentration history in the Fenton-like stage at different pH values. For the experimental conditions please refer to Table 1.

(through reaction between Fe^{3+} and H_2O_2) is inhibited, because the formation of Fe^{3+}-peroxocomplexes (as intermediates) decreases [32]. At pH above 3.5 performance significantly decreases, mainly because the dissolved fraction of iron species decreases [33]. Actually, at high pH values Fe(III) precipitates, therefore decreasing the concentration of dissolved Fe(III). Consequently, the concentration of Fe(II) species also decreases because iron(III) hydroxides are much less reactive than dissolved Fe(III) species towards H_2O_2. The process performance is then affected because a smaller steady-state concentration of hydroxyl radicals is attained.

It is worth noting that two experiments performed at pH 3.0 provided k_{ap} values that differ only 2.7% (average relative error).

3.2.2. Effect of the chloride anion concentration

Inorganic anions (Cl^-, SO_4^{2-}, $H_2PO_4^-/HPO_4^{2-}$, etc.) present in wastewater may have a significant effect on the overall reaction rates of the Fenton process [34]. Moreover, textile effluents contain a large number of inorganic salts [35], and inorganic anions, such as chloride ions, are very common in most wastewaters [36]. Therefore, it is important to evaluate their effect on the process performance.

The effect of the chloride anion (Cl^-) on the O-II degradation by Fenton's reagent was thus investigated and the results are shown in Table 1. It can be seen that the oxidation power of the Fenton process was decreased in the presence of Cl^-, as revealed by its effect on the kinetic constant associated with the reaction between O-II and $HO^\bullet$ species (k_{ap}). The reason for this might therefore be attributed to a decrease in the amount of hydroxyl radicals available as a consequence of the following scavenging reactions [11]:

$$Cl^- + HO^\bullet \rightarrow ClHO^{\bullet -} \quad (11)$$

$$ClHO^{\bullet -} + Fe^{2+} \rightarrow Cl^- + OH^- + Fe^{3+} \quad (12)$$

Consequently, an increase in the chloride anions concentration (at least up to 4 mM) leads to a smaller steady-state hydroxyl radicals concentration, and thus smaller k_{ap} values.

This inhibitory effect is in agreement with others reported in the literature for 2,4-dichlorophenol [37], O-II [38] and other dyes [39], although some authors point for other parallel reactions between Cl anions and other species [34,38]. Finally, it is worth mentioning that Malik and Saha [11] reported that the presence of Cl^- on direct dyes oxidation decreases the extent of degradation, when Cl^- concentration ranges similar to those used in this work were employed.

The effect of the remaining operating variables will now be addressed, to establish the reaction rate equation, in absence of chloride ions and at the optimal pH of 3.

Table 1
Effect of initial pH, chloride ion, dye, hydrogen peroxide or ferrous ion concentrations and temperature on the apparent pseudo first-order rate constant (k_{ap}).

Run	pH	C_{Cl^-} (M)	C_{OII_o} (M)	$C_{H_2O_2\,o}$ (M)	$C_{Fe_o^{2+}}$ (M)	T (K)	k_{ap} (s^{-1})
1	2.0	0	5.0×10^{-5}	2.0×10^{-4}	5.0×10^{-6}	303	2.5×10^{-5}
2	3.0						1.1×10^{-4}
3	3.0						1.1×10^{-4}
4	4.0						7.3×10^{-5}
5	3.0	0	5.0×10^{-5}	2.0×10^{-4}	5.0×10^{-6}	303	1.1×10^{-4}
6		1.0×10^{-3}					7.3×10^{-5}
7		4.0×10^{-3}					4.9×10^{-5}
8		1.0×10^{-2}					5.8×10^{-5}
9	3.0	0	1.1×10^{-4}	2.0×10^{-4}	5.0×10^{-6}	303	6.7×10^{-5}
10			5.9×10^{-5}				9.7×10^{-5}
11			5.1×10^{-5}				1.1×10^{-4}
12			4.1×10^{-5}				1.2×10^{-4}
13			3.2×10^{-5}				1.6×10^{-4}
14	3.0	0	5.0×10^{-5}	1.0×10^{-4}	5.0×10^{-6}	303	7.4×10^{-5}
15				2.0×10^{-4}			9.8×10^{-5}
16				4.0×10^{-4}			1.6×10^{-4}
17				6.0×10^{-4}			3.1×10^{-4}
18				8.0×10^{-4}			3.2×10^{-4}
19				1.0×10^{-3}			4.0×10^{-4}
20	3.0	0	5.1×10^{-5}	2.0×10^{-4}	2.5×10^{-6}	303	4.7×10^{-5}
21					5.0×10^{-6}		1.1×10^{-4}
22					1.0×10^{-5}		4.0×10^{-4}
23					1.5×10^{-5}		5.8×10^{-4}
24					2.0×10^{-5}		8.3×10^{-4}
25	3.0	0	5.3×10^{-5}	2.0×10^{-4}	5.0×10^{-6}	283	2.0×10^{-5}
26						293	5.3×10^{-5}
27						303	1.1×10^{-4}
28						313	2.2×10^{-4}
29						323	4.2×10^{-4}

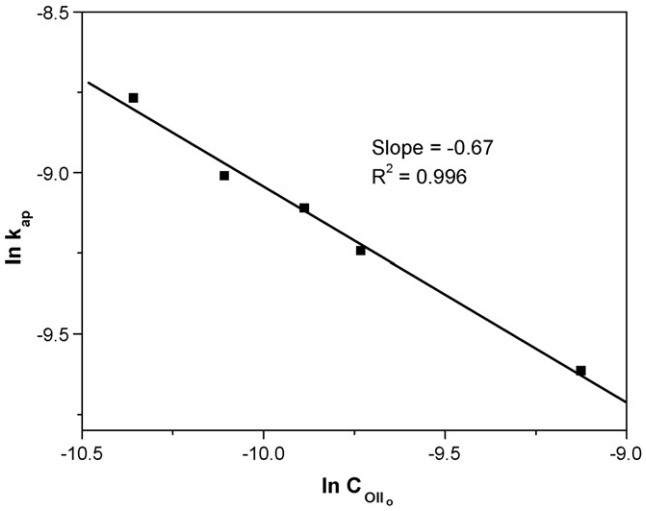

Fig. 3. Effect of the initial dye concentration on the apparent rate constant of O-II degradation. For the experimental conditions please refer to Table 1.

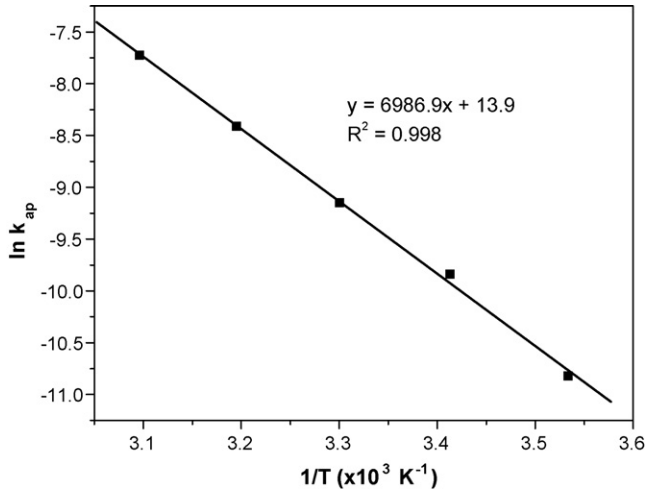

Fig. 4. Arrhenius plot of the apparent rate constant of O-II degradation. For the experimental conditions please refer to Table 1.

3.2.3. Effect of the initial Orange II concentration

The effect of the initial dye concentration was tested at constant initial H_2O_2 and Fe^{2+} concentrations, 2×10^{-4} and 5×10^{-6} M, respectively, with $T = 303$ K and initial pH 3 (data not shown for brevity). The same procedure as above described, applied in the Fenton-like stage (see Fig. 2), allowed obtaining the apparent kinetic constants reported in Table 1 (runs 9–13). Results show that the degradation rate decreases for increasing C_{OII_o}, in the chosen range. The apparent rate order for the dye was then determined to be −0.67 from a $\ln k_{ap}$ vs. $\ln C_{OII_o}$ plot (Fig. 3). The negative effect of the parent organic compound on the apparent kinetic constant was also reported by other authors [e.g., 26,27]. Because the amount of hydrogen peroxide molecules available is the same, this indicates that the higher the dye concentration in the reactor, the smaller is the hydroxyl radicals concentration at steady-state.

3.2.4. Effect of the initial hydrogen peroxide concentration

The effect of the initial hydrogen peroxide concentration ($C_{H_2O_{2o}}$) on k_{ap} can be observed in runs 14–19 (Table 1), and the results show that the degradation rate increases for increasing hydrogen peroxide loads, in the range studied. This trend was expectable. However, the authors found previously [30] that when the value of $C_{H_2O_{2o}}$ is very high, the degradation efficiency keeps constant or even decreases. The fact that in some conditions very high H_2O_2 concentration values lead to a decrease in the final discolouration and rate of degradation is possibly due to the competition between these species for hydroxyl radicals (scavenging effect, Eq. (4)). Indeed, HO radicals are quite non-selective, reacting with the organic matter present but also with other species. De Laat and Gallard [16] have also stated that when the molar ratio $C_{H_2O_{2o}}/C_{Fe_o^{2+}}$ is very high (>500), a detrimental effect might be observed. This was not observed in this work where much lower ratios have been employed (<200).

The apparent rate order regarding the initial H_2O_2 concentration was determined to be 0.77 from an $\ln k_{ap}$ vs. $\ln C_{H_2O_{2o}}$ plot.

3.2.5. Effect of the initial ferrous ion concentration

The procedure described above was also applied to analyze the effect of $C_{Fe_o^{2+}}$ (Table 1). Data obtained put into evidence that the degradation rate is very sensitive to the iron concentration, because it acts as catalyst in the Fenton or Fenton-like process. In the range used, i.e., 2.5×10^{-6} M $< C_{Fe_o^{2+}} < 2.0 \times 10^{-5}$ M and $10 < C_{H_2O_{2o}}/C_{Fe_o^{2+}} < 80$ (mol), the degradation rate increases with the ferrous iron content. Other authors found that, if the ratio $C_{H_2O_{2o}}/C_{Fe_o^{2+}}$ is between 50 and 500, k_{ap} increases linearly with $C_{Fe_o^{2+}}$ [16]. The rate order for the initial Fe^{2+} dose was determined to be 1.43.

3.2.6. Effect of the temperature

The temperature effect on k_{ap} can be observed in runs 25–29, with constant C_{OII_o}, $C_{H_2O_{2o}}$, pH and $C_{Fe_o^{2+}}$ (Table 1). It is observed that the temperature has a strong effect on the O-II degradation rate, which is increased at high temperatures due to an increment in the pseudo first-order rate constant. The data exhibit Arrhenius-type behaviour, with apparent activation energy of 58.1 kJ mol^{-1}, calculated from the usual $\ln k_{ap}$ vs. $1/T$ plot (Fig. 4). The value obtained is very similar to that previously reported by the authors of this work when using a Fe-impregnated activated carbon (56.1 kJ mol^{-1}) [40]. It is interesting to note that such activation energies are somewhat higher than the values measured for: (i) photo-assisted catalytic decomposition of O-II through a Fe/C structured solid (43.55 kJ mol^{-1}) [41] and (ii) photo-Fenton reactions for O-II degradation on structured C-Nafion/Fe-ion surfaces (41.03 kJ mol^{-1}) [42]. Because the activation energy (E_a) obtained for the homogenous system is rather similar to that observed in a heterogeneous process (using the same dye), the reason for the smaller E_a values in the heterogeneous photo-Fenton processes might be attributed to the use of radiation.

3.2.7. Rate equation for the degradation of O-II in a batch reactor

The rate equation can be expressed in a simple way (pseudo first-order), as shown in Eq. (8), wherein k_{ap} depends on the initial conditions as follows:

$$k_{ap} = A C_{OII_o}{}^{a} C_{H_2O_{2o}}{}^{b} C_{Fe_o^{2+}}{}^{c} \exp\left(-\frac{E_a}{RT}\right) \quad (13)$$

where E_a is the apparent activation energy for O-II degradation and the exponents a, b and c represent the apparent reaction orders for O-II, H_2O_2 and Fe^{2+}, respectively. The pre-exponential coefficient A was then calculated by regression minimising the sum of the square residues between k_{ap} data obtained from Eqs. (9) and (13), for each experiment. The value obtained with this procedure was $A = 4.06 \times 10^{13}$ s^{-1} and the resulting parity plot is shown in Fig. 5, evidencing a good agreement between the data computed from both equations. Concluding, the power-law equation for the apparent rate constant of O-II oxidation via Fenton's reagent, in the

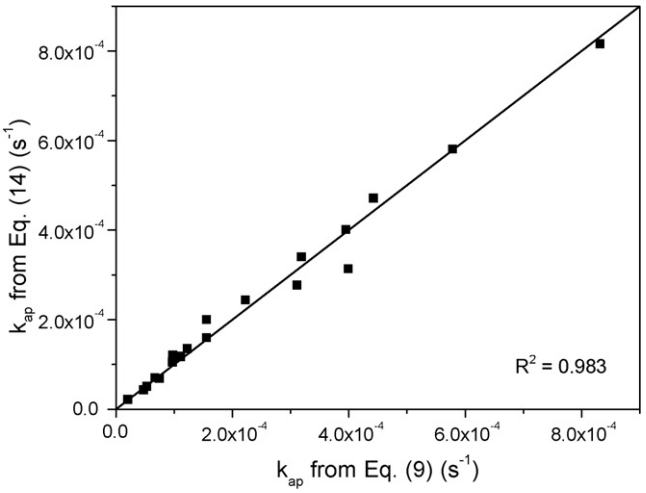

Fig. 5. Plot of k_{ap} obtained from Eq. (9) and predicted from Eq. (14).

Fenton-like stage, is given by:

$$k_{ap} = 4.06 \times 10^{13} C_{OII_o}{}^{-0.67} C_{H_2O_2\,o}{}^{0.77} C_{Fe_o^{2+}}{}^{1.43} \exp\left(-\frac{58092}{RT}\right) \quad (14)$$

Up to now we have established a first-order rate law for O-II degradation, which can be useful for predicting the pseudo steady-state (i.e., when Fe is essentially at the 3+ oxidation state) in a chemical reactor. Obviously, in a batch system this can fail (and really does, as shown below), depending on the initial conditions and extension of the initial (Fenton) phase, which in most experiments performed is short. However, it can be valuable to predict the behaviour of open reactors, operating at steady-state conditions, if the residence time is enough so that Fe^{2+} is almost completely converted into Fe^{3+}.

To predict the dye concentration history in the batch reactor, the mass balance yields the typical exponential curve (Eq. (9)), where k_{ap} is computed from Eq. (14). Fig. 6A–D shows the transient curves in which experimental and model results are compared, for the main parameters studied in this work. In most runs there is an underprediction of the model, which has also some problems in predicting the initial data, as expected (Fenton stage). It is worth

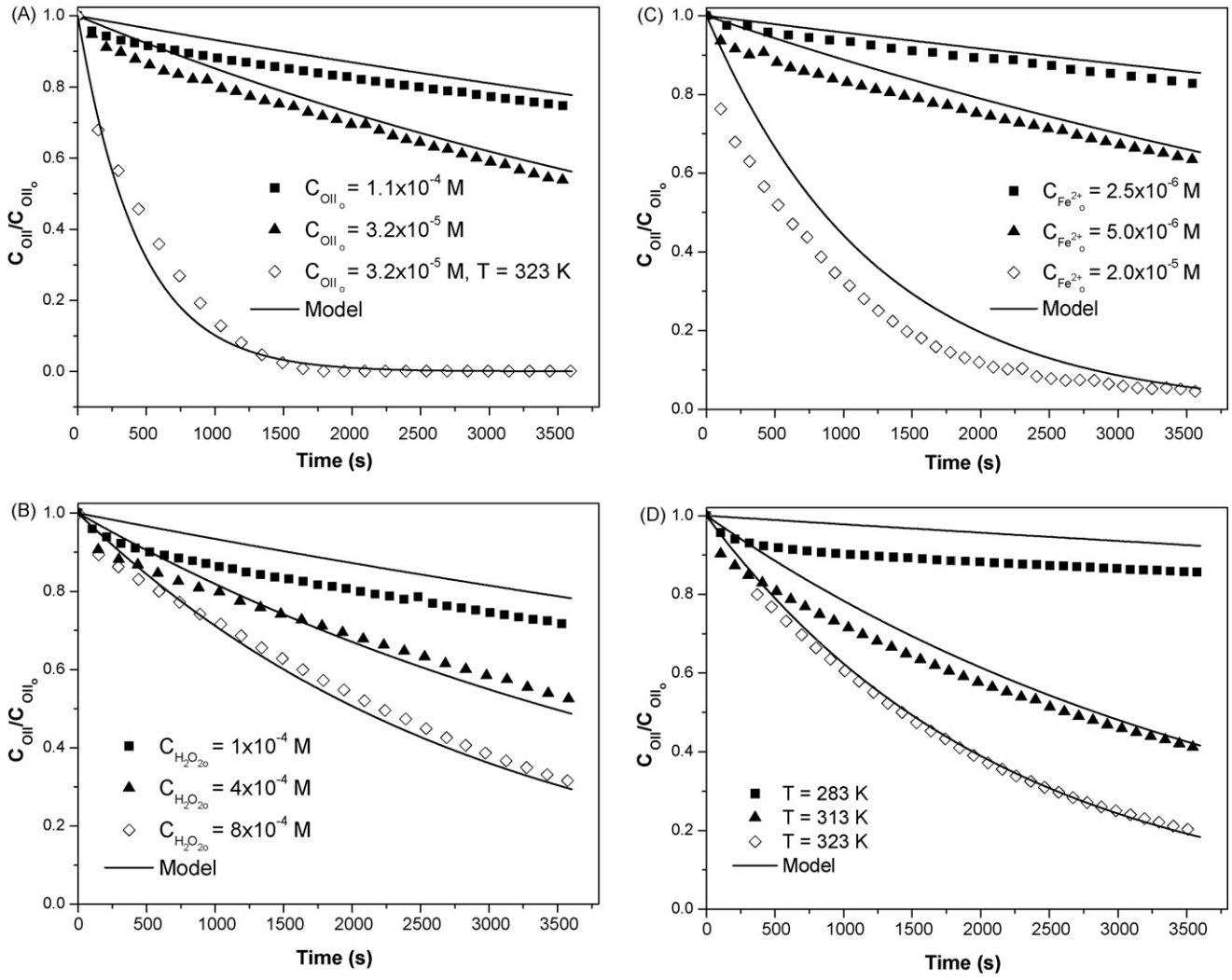

Fig. 6. Orange II concentration histories when changing: (A) C_{OII_o}; (B) $C_{H_2O_2\,o}$; (C) $C_{Fe_o^{2+}}$; and (D) the temperature. For the experimental conditions please refer to Table 1.

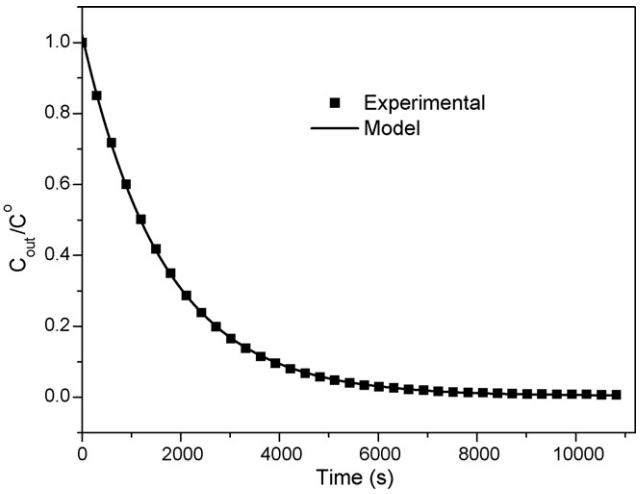

Fig. 7. Typical experimental data (Danckwerts' *C* curve) for a tracer experiment and corresponding model fit. Flow rate = 0.58 ml s^{-1}.

noting that the model has a better accuracy when a fast transition from stage I to stage II is ensured. This means high concentration of hydrogen peroxide (average absolute error of 4.9% vs. 6.5% for the lowest concentration, Fig. 6B) or high temperature (average absolute error of 1.2% vs. 7.0% for the lowest temperature, Fig. 6D), which is in good agreement with Eq. (10). In Fig. 6A the concentration of O-II was varied, but again for simplicity only two experiments are shown in the graphic, corresponding to the highest and lowest dye concentrations used. An additional run was still carried out at a higher temperature, putting into evidence the better adherence of the model under such conditions.

3.3. Continuous stirred tank reactor (CSTR) experiments

In an ideal CSTR (or perfectly mixed reactor), the contents are well-stirred and uniform throughout; therefore the exit stream has the same composition as the fluid within the vessel. Tracer experiments have confirmed that the reactor used in this work closely matches these ideal mixing conditions. This is evidenced in Fig. 7, where the theoretical curve is given by the typical Danckwerts' *C* curve, i.e., the normalized response to a pulse input [43,44]:

$$C(t) = \frac{C_{out}(t)}{C^o} = \exp\left(-\frac{t}{\tau}\right) \quad (15)$$

For a CSTR, the space-time in Eq. (15) is equal to the mean residence time. The differences between the residence times obtained from the fit to experimental tracer data and the formula value ($\tau = V/Q$) are between 2.4% and 5.0%, for different flow rates in the ranges of the oxidation experiments (data not shown).

Table 2 shows the conditions of the Fenton's experiments carried out in the continuous reactor. In this case, the inlet O-II, H_2O_2 and Fe^{2+} concentrations, temperature and residence time were changed, within the ranges used in the batch reactor. However, experiments out of such range were also performed, shown in the same table. Experimental and model predictions, in terms of dye conversions, are also reported, which have been calculated as follows:

$$X = \frac{C_{OII_{in}} - C_{OII_{out}}}{C_{OII_{in}}} \times 100 \quad (16)$$

where $C_{OII_{in}}$ is the inlet O-II concentration and $C_{OII_{out}}$ the outlet one.

In Figs. 8–12 is shown the effect of the reagents concentrations (at the reactor inlet), temperature and residence time on the steady-state conversion. In all of them, closed symbols refer to conditions

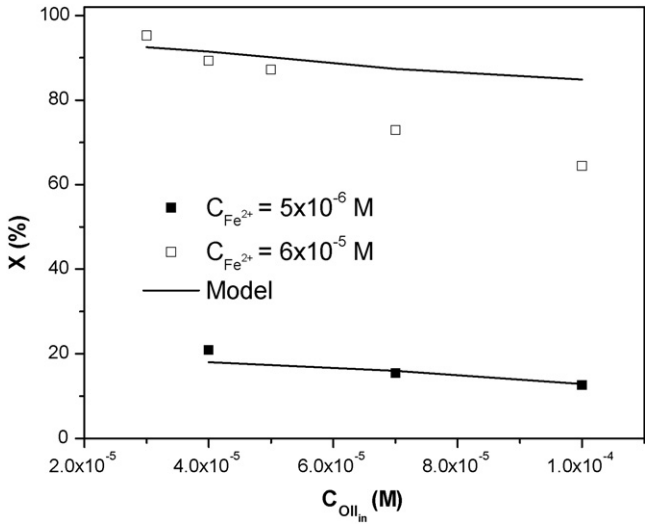

Fig. 8. Effect of the inlet dye concentration on the steady-state O-II conversion in the continuous reactor. For the experimental conditions please refer to Table 2.

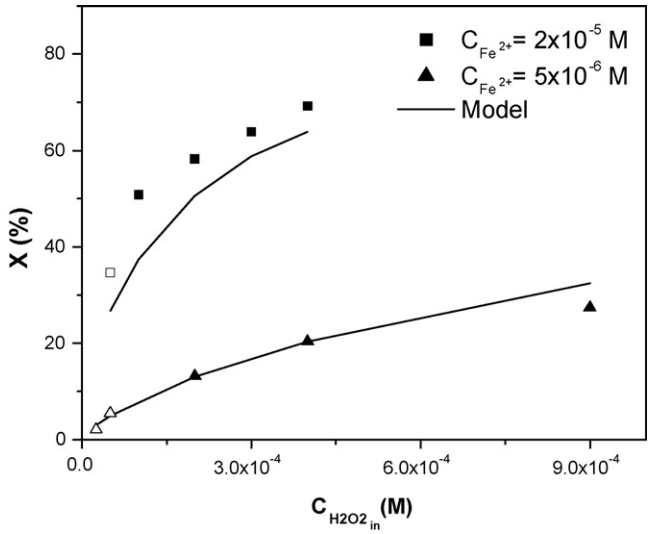

Fig. 9. Effect of the inlet H_2O_2 concentration on the steady-state O-II conversion in the continuous reactor. For the experimental conditions please refer to Table 2.

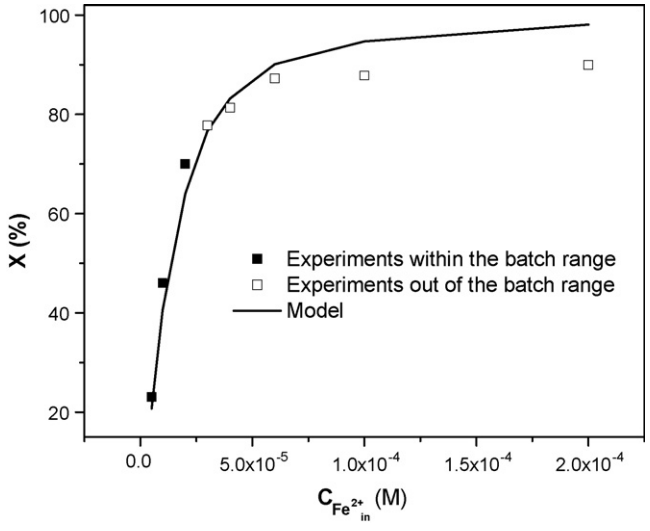

Fig. 10. Effect of the inlet Fe^{2+} concentration on the steady-state O-II conversion in the continuous reactor. For the experimental conditions please refer to Table 2.

Table 2
Experimental and model prediction of O-II conversion in the continuous stirred tank reactor.

Run	$C_{OII_{in}}$ (M)	$C_{H_2O_{2in}}$ (M)	$C_{Fe_{in}^{2+}}$ (M)	τ (s)	T (K)	X_{exp} (%)	X_{mod} (%)
1	4.0×10^{-5}			1136.7		18.0	21.0
2	7.0×10^{-5}	4.0×10^{-4}	5.0×10^{-6}	1142.2	303	16.0	15.5
3	1.0×10^{-4}			1147.2		12.9	12.7
4		4.0×10^{-4}		1221.6	303	69.2	64.0
5		3.0×10^{-4}		1222.7		63.8	58.7
6	5.0×10^{-5}	2.0×10^{-4}	2.0×10^{-5}	1199.7		58.3	50.6
7		1.0×10^{-4}		1195.8		50.8	37.4
8		5.0×10^{-5}		1238.1		34.6	26.7[a]
9		2.5×10^{-5}		1284.3		2.1	3.0[a]
10		5.0×10^{-5}		1284.3		5.5	5.0[a]
11	5.0×10^{-5}	2.0×10^{-4}	5.0×10^{-6}	1268.3	303	13.2	13.0
12		4.0×10^{-4}		1268.3		20.3	20.3
13		9.0×10^{-4}		1278.3		27.4	32.4
14			5.0×10^{-6}	1302.3		23.1	20.7
15	5.0×10^{-5}	4.0×10^{-4}	1.0×10^{-5}	1265.4	303	46.0	40.6
16			2.0×10^{-5}	1221.6		70.0	64.0
17				1284.3	288	9.2	7.2
18	5.0×10^{-5}	4.0×10^{-4}	5.0×10^{-6}	1284.3	318	46.3	43.4
19				1268.3	333	71.5	67.0[a]
20				1136.7	303	18.0	21.0
21	5.0×10^{-5}	4.0×10^{-4}	5.0×10^{-6}	1485.5		25.3	25.7
22				2341.3		36.8	35.3
23	3.0×10^{-5}			1247.1		95.3	92.4[a]
24	4.0×10^{-5}			1302.3		89.3	91.5[a]
25	5.0×10^{-5}	4.0×10^{-4}	6.0×10^{-5}	1302.3	303	87.2	90.1[a]
26	7.0×10^{-5}			1247.1		72.9	87.4[a]
27	1.0×10^{-4}			1247.1		64.5	84.8[a]
28			3.0×10^{-5}	1265.0		77.8	76.6[a]
29			4.0×10^{-5}	1265.4		81.4	83.2[a]
30	5.0×10^{-5}	4.0×10^{-4}	6.0×10^{-5}	1302.3	303	87.2	90.1[a]
31			1.0×10^{-4}	1228.7		87.8	94.7[a]
32			2.0×10^{-4}	1302.3		90.0	98.1[a]
33				1238.1	283	75.0	62.9[a]
34				1247.1	296	80.8	83.4[a]
35				1302.3	303	87.2	90.1[a]
36				1247.1	315	89.4	95.5[a]
37				1238.1	323	93.5	97.4[a]
38	5.0×10^{-5}	4.0×10^{-4}	6.0×10^{-5}	1238.1	336	94.6	98.8[a]
39				2054.5	283	77.8	74.6[a]
40				2060.7	299	94.2	91.8[a]
41				2504.3	300	90.2	93.6[a]
42				2476.2	323	96.3	98.7[a]
43				2407.9	334	97.3	99.3[a]
44				1302.3		87.2	90.1[a]
45	5.0×10^{-5}	4.0×10^{-4}	6.0×10^{-5}	1760.6	303	88.9	92.5[a]
46				2504.3		90.2	94.6[a]

[a] Refers to the runs out of the batch reactor range studied.

within the batch range, whereas open symbols to values out of it. It can be concluded that the effect of each parameter on O-II conversion is similar to that observed in the batch reactor. First, O-II conversion decreases when the dye concentration in the reactor feed increases (see Fig. 8). In terms of hydrogen peroxide concentration (Fig. 9), it is evident that when the H_2O_2 concentration is increased in the feed, an increment in the O-II conversion is noticed, because more hydroxyl radicals are available for oxidation, in the range studied. The same behaviour is observed when the ferrous ion is changed, as showed in the previous figures and also in Fig. 10. In the latter, an increase in the Fe^{2+} load fed to the reactor from 5×10^{-6} to 6×10^{-5} M leads to an increase in the steady-state O-II conversion from 23% to 87%, however runs carried out at higher Fe^{2+} doses ($1–2 \times 10^{-4}$ M) resulted in no appreciable differences in terms of O-II removal (up to 90%). Temperature effect was investigated in the range 283–336 K, showing to be an important parameter in the Fenton's process (Fig. 11), particularly when low catalyst doses are employed. Finally, when the residence time was incremented, better results were obtained in terms of O-II conversion at steady-state, as expected (see Fig. 12).

3.4. Validation of the model in the continuous reactor

From a simple mass balance to the CSTR, at steady-state, one can write:

$$F_{OII_{in}} = F_{OII_{out}} + (-r_{OII})_{out} V \tag{17}$$

where $F_{OII_{in}}$ and $F_{OII_{out}}$ denote the dye molar flow rates at the reactor inlet and outlet, respectively. Since the reaction is of pseudo first-order type (Eq. (8)), the outlet concentration of O-II can be given by:

$$C_{OII_{out}} = \frac{C_{OII_{in}}}{1 + k_{ap}\tau} \tag{18}$$

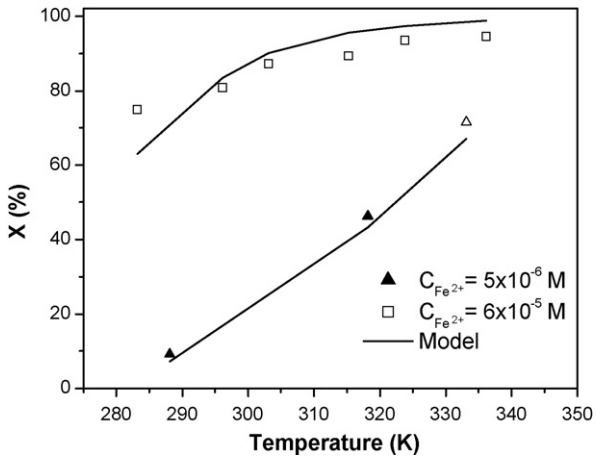

Fig. 11. Effect of the temperature on the steady-state O-II conversion in the continuous reactor. For the experimental conditions please refer to Table 2.

where $\tau = V/Q$ is the space-time, V is the reactor volume (0.92 L) and Q is the total flow rate. k_{ap} is obtained by Eq. (14), based on the concentration of each species at the reactor inlet, because these are the conditions that determine the steady-state radicals concentration. This issue can also be rationalized from the well-known total segregation model [43,44], which assumes that all fluid elements having the same age (residence time) "travel together" in the reactor and do not mix with elements of different ages, until they exit the reactor. Because there is no interchange of matter between fluid elements, each one acts as a batch reactor and so the mean steady-state conversion in the reactor is given by:

$$X = \int_{o}^{\infty} X_{batch}(t)\ E(t)\,dt \tag{19}$$

where $X_{batch}(t)$ refers to the transient conversion equation in a batch reactor ($X_{batch} = 1 - e^{(-k_{ap}t)}$, because the reaction is pseudo first-order – Eq. (9)), and $E(t)$ is the residence time distribution function ($E(t) = (C(t)/\tau) = (1/\tau)\exp(-(t/\tau))$, see Eq. (15)). What is important to remark is that, in this model, computation of conversion in a continuous reactor by Eq. (19) makes use of an expression for a "micro" batch reactor that is based on the reactor feed conditions.

The model conversion (X_{mod}) was then obtained using Eqs. (16) and (18) (the total segregation model yields the same value, because the reaction is pseudo first-order – linear system). Figs. 8–12 show the model predictions for all the experiments performed.

In what concerns the effect of the inlet O-II concentration (Fig. 8), it is remarkable the adherence of the model to experimental data in which iron concentrations within the range used in the batch runs have been employed (closed symbols, maximum absolute error of 3%). However, even when catalyst doses one order of magnitude higher are employed, the model is able to predict the negative effect of increasing dye concentrations, although with higher deviations. This negative effect is related with a decrease in the number of oxidant molecules (or radicals) available per dye molecule (lower H_2O_2/O-II ratios).

The model fits also reasonably data obtained in experiments where increasing oxidant dosages were employed (Fig. 9), particularly for low iron loads. The model adherence is however worst when the catalyst concentration approaches the upper limit employed in the kinetic study (2×10^{-5} M). The difficulty in predicting conversions under experimental conditions in the limits of the range employed in the kinetic study is also evident in terms of hydrogen peroxide concentrations. This can be seen in the first data series, for lower Fe^{2+} loads (last data), because the radicals scavenging effect that occurs at high oxidant loads (cf. Eq. (4)) is not taken into account in the power-law type rate equation.

Fig. 10 reinforces what was said in the previous paragraph, i.e., the good adherence of the model to experimental data when using conditions (now iron concentrations) within those employed when establishing the rate equation. However it has some difficulties to predict the scavenging effect, i.e., the parallel and undesirable reaction that occurs between the catalyst and the hydroxyl radicals (Eq. (2)) at high Fe loads.

Results obtained when the temperature and residence time were changed (Figs. 11 and 12, respectively) show that the model also predicts well the positive effect of both parameters; this applies particularly for low iron loads, and even reasonably when iron concentrations above those employed in the kinetic study were used.

Finally, in Fig. 13 is shown the comparison between experimental conversion data and model predictions, for all the experiments of Table 2. In the parity plot it is observed that there is reasonably good adherence of the model, in spite no fitting parameters exist. The more significant deviations concern experiments performed

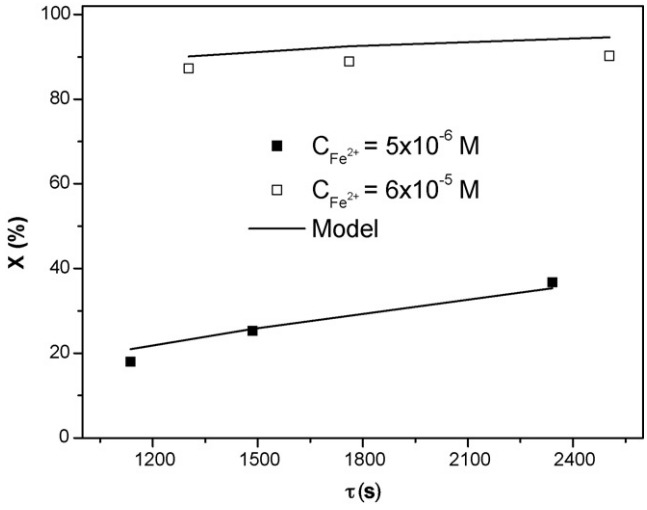

Fig. 12. Effect of the space-time on the steady-state O-II conversion in the continuous reactor. For the experimental conditions please refer to Table 2.

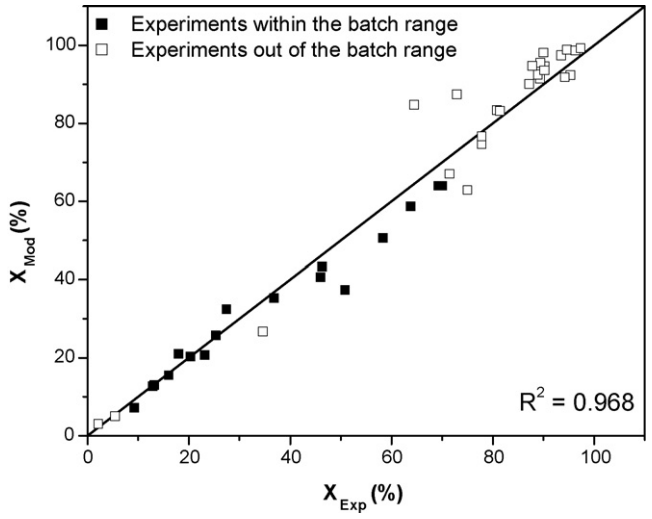

Fig. 13. Parity plot comparing O-II conversion obtained experimentally vs. O-II conversion predicted by the CSTR model.

off the kinetic study range (e.g., runs 26 and 27, absolute errors of 15% and 20%, respectively), although on average predictions differ less than 5%. The model revealed, therefore, to be effective for predicting experiments carried out within the range used in the batch reactor or out of it, the later being performed also with the goal of extending the O-II conversion range.

4. Conclusions

Performances reached during Orange II degradation by means of Fenton's reagent highly depend on the operating conditions, i.e., reagents dosage, temperature, pH and time of reaction (batch reactor) or residence time (continuous reactor).

In this study, and particularly in the batch reactor experiments, low concentrations of hydrogen peroxide and ferrous ion were applied to eliminate the useless use of excessive reagent doses, commonly found at high Fe^{2+} and/or H_2O_2 doses. Depending on the initial conditions, about 14–95% of O-II was removed in 1 h.

Experiments carried out in the batch reactor evidenced that optimum pH is around 3 and the negative effect of Cl^- species. It was also observed the positive effects of increasing the reaction temperature, H_2O_2 or Fe^{2+} concentrations, and the negative effect of increasing dye concentrations, trends that are in accordance with experiments performed in the CSTR.

The dye concentration history showed a change in the kinetics, typical of this process, being initially very rapid (Fenton stage) and afterwards the slower Fenton-like stage proceeds, where iron is mostly in the 3+ oxidation state. For the longer and last stage, a pseudo steady-state approach was employed to deduce the reaction rate, which was found to be of the first-order type with respect to O-II concentration. The dependence of the apparent kinetic constant on the initial operating conditions was then deduced, leading to a power-law rate equation with Arrhenius dependency (apparent activation energy of 58.1 kJ mol^{-1}). In experiments carried out in duplicate, k_{ap} varied by less than 10%.

This rate equation revealed to be somewhat useful to predict dye concentration histories in the batch reactor (based on the known initial conditions) and steady-state dye conversion in the CSTR (based on inlet conditions), wherein Fe is essentially at the 3+ oxidation state. However, under certain conditions, some underprediction was observed.

A large set of experiments was performed in the continuous reactor, to analyze the effects of all variables involved. In all cases, it was observed a reasonably good agreement between experimental and model results, even for experiments performed out of the ranges used in the batch kinetic study. It is important to remark the ability of the model to predict data in a wide range of dye conversions values, from 2% to 97%.

Acknowledgements

The authors deeply acknowledge Profs. Adélio Mendes and Jorge Martins, from LEPAE – FEUP, for their fruitful suggestions and discussions. J. Herney Ramirez wishes to express his gratitude to FCT for the PhD grant (ref.: SFRH/BD/24435/2005).

References

[1] M.S. Lucas, A.A. Dias, A. Sampaio, C. Amaral, J.A. Peres, Degradation of a textile reactive Azo dye by a combined chemical–biological process: Fenton's reagent-yeast, Water Res. 41 (2007) 1103–1109.
[2] C.M. Carliell, S.J. Barclay, N. Naidoo, C.A. Buckely, D.A. Mulholland, E. Senior, An investigation into the reduction of azo dyes by anaerobic microorganisms, Water S.A. 21 (1995) 61–69.
[3] C. Rafols, D. Barcelo, Determination of mono- and disulphonated azo dyes by liquid chromatography–atmospheric pressure ionization mass spectrometry, J. Chromatogr. A 777 (1997) 177–192.
[4] P.C. Vandevivere, R. Bianchi, W. Verstraete, Review: treatment and reuse of wastewater from the textile wet-processing industry: review of emerging technologies, J. Chem. Technol. Biotechnol. 72 (1998) 289–302.
[5] M. Stylidi, D.I. Kondarides, X.E. Verykios, Pathways of solar light-induced photocatalytic degradation of azo dyes in aqueous TiO_2 suspensions, Appl. Catal. B: Environ. 40 (2003) 271–286.
[6] C. Gomes da Silva, J.L. Faria, Degradation of an azo dye in aqueous solution by UV irradiation, J. Photochem. Photobiol. A 155 (2003) 133–143.
[7] M.A. Brown, S.C. De Vito, Predicting azo dye toxicity, Crit. Rev. Environ. Sci. Technol. 23 (1993) 249–324.
[8] D. Méndez-Paz, F. Omil, J.M. Lema, Anaerobic treatment of azo dye Acid Orange 7 under fed-batch and continuous conditions, Water Res. 39 (2005) 771–778.
[9] K. Dutta, S. Mukhopadhyay, S. Bhattacharjee, B. Chaudhuri, Chemical oxidation of methylene blue using a Fenton-like reaction, J. Hazard. Mater. 84 (2001) 57–71.
[10] K. Swaminathan, S. Sandhya, A.C. Sophia, K. Pachhade, Y.V. Subrahmanyam, Decolorization and degradation of H-acid and other dyes using ferrous–hydrogen peroxide system, Chemosphere 50 (2003) 619–625.
[11] P.K. Malik, S.K. Saha, Oxidation of direct dyes with hydrogen peroxide using ferrous ion as catalyst, Sep. Purif. Technol. 31 (2003) 241–250.
[12] S.H. Lin, C.C. Lo, Fenton process for treatment of desizing wastewater, Water Res. 31 (1997) 2050–2056.
[13] R.J. Bigda, Consider Fenton chemistry for wastewater treatment, Chem. Eng. Prog. 91 (1995) 62–66.
[14] C. Walling, Fenton's reagent revisited, Acc. Chem. Res. 8 (1975) 125–131.
[15] F.J. Rivas, V. Navarrete, F.J. Beltran, J.F. Garcia-Araya, Simazine Fenton's oxidation in a continuous reactor, Appl. Catal. B: Environ. 48 (2004) 249–258.
[16] J. De Laat, H. Gallard, Catalytic decomposition of hydrogen peroxide by Fe(III) in homogeneous aqueous solution: mechanism and kinetic modeling, Environ. Sci. Technol. 33 (1999) 2726–2732.
[17] D.D. Dionysiou, M.T. Suidan, I. Baudin, J.M. Laîne, Effect of hydrogen peroxide on the destruction of organic contaminants-synergism and inhibition in a continuous-mode photocatalytic reactor, Appl. Catal. B: Environ. 50 (2004) 259–269.
[18] E.S. Henle, Y. Luo, S. Linn, Fe^{2+}, Fe^{3+}, and oxygen react with DNA-derived radicals formed during iron-mediated Fenton reactions, Biochemistry 35 (1996) 12212–12219.
[19] F.J. Rivas, F.J. Beltran, J. Frades, P. Buxeda, Oxidation of p-hydroxybenzoic acid by Fenton's reagent, Water Res. 35 (2001) 387–396.
[20] R. Chen, J.J. Pignatello, Role of quinone intermediates as electron shuttles in Fenton and photoassisted Fenton oxidations of aromatic compounds, Environ. Sci. Technol. 31 (1997) 2399–2406.
[21] W.R. Haag, C.C.D. Yao, Rate constants for reaction of hydroxyl radicals with several drinking water contaminants, Environ. Sci. Technol. 26 (1992) 1005–1013.
[22] H. Zhang, H.J. Choi, C.P. Huang, Treatment of landfill leachate by Fenton's reagent in a continuous stirred tank reactor, J. Hazard. Mater. 136 (2006) 618–623.
[23] S.Y. Oh, P.C. Chiu, B.J. Kim, D.K. Cha, Enhancing Fenton oxidation of TNT and RDX through pretreatment with zero-valent iron, Water Res. 37 (2003) 4275–4283.
[24] J.H. Ramirez, C.A. Costa, L.M. Madeira, G. Mata, M.A. Vicente, M.L. Rojas-Cervantes, A.J. Lopez-Peinado, R.M. Martin-Aranda, Fenton-like oxidation of Orange II solutions using heterogeneous catalysts based on saponite clay, Appl. Catal. B: Environ. 71 (2007) 44–56.
[25] H. Gallard, J. De Laat, Kinetic modelling of Fe(III)/H_2O_2 oxidation reactions in dilute aqueous solution using atrazine as a model organic compound, Water Res. 34 (2000) 3107–3116.
[26] J.H. Sun, S.P. Sun, M.H. Fan, H.Q. Guo, L.P. Qiao, R.X. Sun, A kinetic study on the degradation of p-nitroaniline by Fenton oxidation process, J. Hazard Mater. 148 (2007) 172–177.
[27] M.L. Rodriguez, V.I. Timokhin, S. Contreras, E. Chamarro, S. Esplugas, Rate equation for the degradation of nitrobenzene by 'Fenton-like' reagent, Adv. Environ. Res. 7 (2003) 583–595.
[28] M.J. Liou, M.C. Lu, Catalytic degradation of nitroaromatic explosives with Fenton's reagent, J. Mol. Catal. A: Chem. 277 (2007) 155–163.
[29] M.E. Lindsey, M.A. Tarr, Inhibited hydroxyl radical degradation of aromatic hydrocarbons in the presence of dissolved fulvic acid, Water Res. 34 (2000) 2385–2389.
[30] J.H. Ramirez, C.A. Costa, L.M. Madeira, Experimental design to optimize the degradation of the synthetic dye Orange II using Fenton's reagent, Catal. Today 107–108 (2005) 68–76.
[31] E. Neyens, J. Baeyens, A review of classic Fenton's peroxidation as an advanced oxidation technique, J. Hazard. Mater. 98 (2003) 33–50.
[32] J.J. Pignatello, Dark and photoassisted iron(3+)-catalyzed degradation of chlorophenoxy herbicides by hydrogen peroxide, Environ. Sci. Technol. 26 (1992) 944–951.
[33] M. Pera-Titus, V. Garcia-Molina, M.A. Baños, J. Gimenez, S. Esplugas, Degradation of chlorophenols by means of advanced oxidation processes: a general review, Appl. Catal. B: Environ. 47 (2004) 219–256.
[34] J. De Laat, T.L. Giang, B. Legube, A comparative study of the effects of chloride, sulfate and nitrate ions on the rates of decomposition of H_2O_2 and organic compounds by Fe(II)/H_2O_2 and Fe(III)/H_2O_2, Chemosphere 55 (2004) 715–723.
[35] G. Chen, X. Chai, P. Yue, Y. Mi, Treatment of textile desizing wastewater by pilot scale nanofiltration membrane separation, J. Membr. Sci. 127 (1997) 93–99.
[36] M.C. Lu, J.N. Chen, C.P. Chang, Effect of inorganic ions on the oxidation of dichlorvos insecticide with Fenton's reagent, Chemosphere 35 (1997) 2285–2293.

[37] W.Z. Tang, C.P. Huang, 2,4-Dichlorophenol oxidation kinetics by Fenton's reagent, Environ. Technol. 17 (1996) 1371–1378.
[38] J. Kiwi, A. Lopez, V. Nadtochenko, Mechanism and kinetics of the OH-radical intervention during Fenton oxidation in the presence of a significant amount of radical scavenger (Cl^-), Environ. Sci. Technol. 34 (2000) 2162–2168.
[39] C. Guillard, H. Lachheb, A. Housa, M. Ksibi, E. Elaloui, J.M. Herrmann, Influence of chemical structure of dyes, of pH and of inorganic salts on their photocatalytic degradation by TiO_2 comparison of the efficiency of powder and supported TiO_2, J. Photochem. Photobiol. A 158 (2003) 27–36.
[40] J.H. Ramirez, F.J. Maldonado-Hodar, A.F. Perez-Cadenas, C. Moreno-Castilla, C.A. Costa, L.M. Madeira, Azo-dye Orange II degradation by heterogeneous Fenton-like reaction using carbon-Fe catalysts, Appl. Catal. B: Environ. 75 (2007) 317–328.
[41] T. Yuranova, O. Enea, E. Mielczarski, J. Mielczarski, P. Albers, J. Kiwi, Fenton immobilized photo-assisted catalysis through a Fe/C structured fabric, Appl. Catal. B: Environ. 49 (2004) 39–50.
[42] S. Parra, I. Guasaquillo, O. Enea, E. Mielczarski, J. Mielczarki, P. Albers, L. Kiwi-Minsker, J. Kiwi, Abatement of an azo dye on structured C-Nafion/Fe-ion surfaces by photo-Fenton reactions leading to carboxylate intermediates with a remarkable biodegradability increase of the treated solution, J. Phys. Chem. B 107 (2003) 7026–7035.
[43] H.S. Fogler, Elements of Chemical Reaction Engineering, 3rd ed., Prentice-Hall, New Jersey, 1999.
[44] A.E. Rodrigues, Theory of residence time distributions, in: A.E. Rodrigues, J.M. Calo, N.H. Sweed (Eds.), Multiphase Chemical Reactors, NATO ASI Series, Sijthoff Noordhoff, 1981.